Coupled Mode Analysis of Two-Dimensional Chiral Grating

Ahmed M. Attiya

Microwave Engineering Department
Electronics Research Institute, El-Tahreer St. Dokki, Giza, Egypt, 12622
aattiya@ksu.edu.sa

Abstract ─ This paper introduces a modal analysis for two-dimensional chiral grating. The grating structure is composed of rectangular chiral rods arranged in rectangular periodic cells and embedded in another chiral base material. Total fields are presented in terms of transverse electric and magnetic field components which are expanded as two sets of TE and TM Floquet modes. This representation is used in Maxwell's curl equations to formulate the problem as an eigenvalue problem. The resulting eigenvalues correspond to the forward and backward propagation coefficients. On the other hand, the eigenvectors correspond to the amplitudes of the TE and TM Floquet modes in the forward and backward propagating modes. Reflection and transmission coefficients of two semi-infinite chiral gratings are obtained by combining this modal analysis and mode matching method. This analysis is extended to obtain the reflection and transmission coefficients of a finite thickness two-dimensional chiral grating slab by using the generalized scattering matrix method.

Index Terms ─ Chiral medium, grating, modal analysis, mode matching.

I. INTRODUCTION

Electromagnetic interaction with periodic structures has significant importance in many applications like filters, frequency selective surfaces, artificial media, etc. This problem can be viewed from different points of view like the amplitude of the reflection and transmission coefficients as in the case of frequency selective surfaces and the phase of the transmitted wave as in the case of artificial metamaterials. Chiral medium introduces an additional point which is the polarization conversion and electro-magnetic coupling. This is the motivation in the present paper and other previously published papers to study electromagnetic wave interaction with periodic chiral structures [1-4]. Guiding properties of infinite multi-layers chiral slab was discussed by using modal analysis. This modal analysis of periodic layered chiral slabs is extended to study the reflection and transmission of a one-dimensional chiral grating slab by using the mode matching method [4].

The present paper extends this modal analysis to study the reflection and transmission of an obliquely incident TE or TM plane wave due to a two-dimensional chiral grating slab as shown in Fig. (1). The slab is composed of rectangular rods implanted inside a base substrate in a rectangular periodic scheme. Similar analysis is discussed by the author with others for both two-dimensional dielectric and two-dimensional magneto-dielectric grating slabs [5-6]. However, the key difference in the present case is the coupling between the electric and magnetic fields due to the chirality coefficient. In dielectric grating and magneto-dielectric grating the formulation begins with the wave equation in the corresponding medium. For these cases, the wave equation is simply a second order differential equation and both electric and magnetic field components are separated. However, in the present case the wave equation in the chiral medium is a fourth order differential equation [7]. Thus, it would be much more complicated to start the present formulation with wave equation as in the cases of dielectric and magneto-dielectric gratings. This is the motivation here to formulate the problem starting from Maxwell's curl equations. Similar analysis is discussed for the problems of chirowaveguides and chirowaveguide discontinuities by using the coupled mode analysis. [8-13]. Method of moments has also been used to simulate transmission of plane waves through an aperture in a conducting plane in the presence of a chiral medium [14]. This method can be extended to simulate the periodic patch or slots on a chiral slab. However, it would be quite complicated to simulate a 2-D grating slab since the problem would be the volume integral equation instead of the simple surface integral equation.

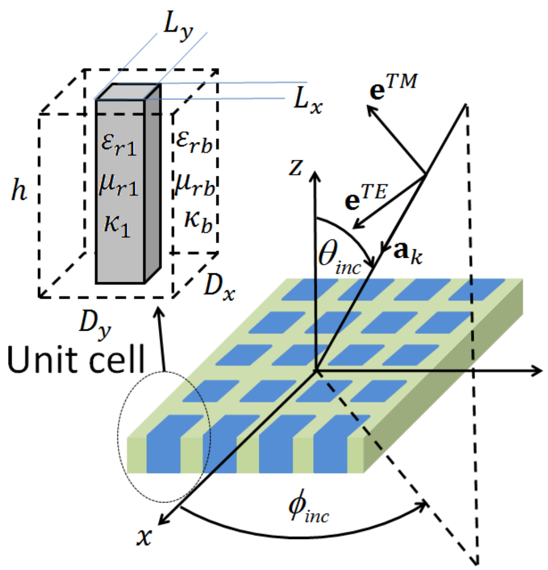

Fig. 1. A two-dimensional chiral grating slab excited by an obliquely incident TE and TM plane waves.

In the following section, the modal analysis of an infinite chiral grating is presented as an eigenvalue problem where the eigenvalues correspond to the complex propagation wave numbers in the longitudinal direction and the eigenvectors represent the transverse field distributions of the different modes in this infinite periodic structure. This modal analysis is combined with the mode matching method to obtain the scattering matrix of a semi-infinite grating. Then the generalized matrix approach combined with complex propagation wave numbers of the different modes in the infinite grating structure are used to obtain the reflection and transmission coefficients of the finite-thickness chiral grating slab. The present analysis represents a generalization to the previously published analysis for one-dimensional chiral grating [4] where the same results of the one-dimensional case can be obtained by extending the length of the implanted rod in y direction L_y to be the same as the cell size in the same direction D_y. These points are discussed in detail in Sec. III in addition to other results and discussions related to the two-dimensional chiral grating slab.

II. THEORY

A. Modal analysis of infinite two-dimensional chiral grating

Total fields inside the chiral grating are divided into transverse and longitudinal components as follows:

$$\mathbf{E}(x,y,z) = \mathbf{E}_t(x,y,z) + E_z(x,y,z)\mathbf{a}_z \ , \qquad (1\text{-a})$$

$$\mathbf{H}(x,y,z) = \mathbf{H}_t(x,y,z) + H_z(x,y,z)\mathbf{a}_z \ . \qquad (1\text{-b})$$

The transverse field components are expanded as an infinite series of bi-orthogonal Floquet TE and TM modes propagating along the longitudinal direction:

$$\mathbf{E}_t = \sum_p \Phi_{(p)}^{TE} \tilde{\mathbf{e}}_{(p)}^{TE}(x,y) e^{-j\beta_{(p)}^{TE} z} + \Phi_{(p)}^{TM} \tilde{\mathbf{e}}_{(p)}^{TM}(x,y) e^{-j\beta_{(p)}^{TM} z}, \qquad (2\text{-a})$$

$$\mathbf{H}_t = \sum_p C_{(p)}^{TE} \tilde{\mathbf{h}}_{(p)}^{TE}(x,y) e^{-j\beta_{(p)}^{TE} z} + C_{(p)}^{TM} \tilde{\mathbf{h}}_{(p)}^{TM}(x,y) e^{-j\beta_{(p)}^{TM} z}, \qquad (2\text{-b})$$

where $\Phi_{(p)}^{TE}$, $\Phi_{(p)}^{TM}$, $C_{(p)}^{TE}$, and $C_{(p)}^{TM}$ are four sets of unknown amplitudes to be determined. $\beta_{(p)}^{TE}$ and $\beta_{(p)}^{TM}$ are the longitudinal propagation constants of the $(p)^{th}$ TE and $(p)^{th}$ TM mode, respectively. For computational purpose, these infinite series are truncated at an upper limit $p = P$ assuming that they start from $p = 1$. The transverse expansion functions of the electric and magnetic fields are given by:

$$\tilde{\mathbf{e}}_{mn}^{TE}(x,y) = T_{mn}\left(k_{yn}\mathbf{a}_x - k_{xm}\mathbf{a}_y\right)/k_{tmn} \ , \qquad (3\text{-a})$$

$$\tilde{\mathbf{e}}_{mn}^{TM}(x,y) = T_{mn}\left(k_{xm}\mathbf{a}_x + k_{yn}\mathbf{a}_y\right)/k_{tmn} \ , \qquad (3\text{-b})$$

$$\tilde{\mathbf{h}}_{mn}^{TE}(x,y) = T_{mn}\left(k_{xm}\mathbf{a}_x + k_{yn}\mathbf{a}_y\right)/k_{tmn} \ , \qquad (3\text{-c})$$

$$\tilde{\mathbf{h}}_{mn}^{TM}(x,y) = T_{mn}\left(-k_{yn}\mathbf{a}_x + k_{xm}\mathbf{a}_y\right)/k_{tmn} \ , \qquad (3\text{-d})$$

where

$$k_{xm} = k_0 \sin\theta_{inc} \cos\phi_{inc} + 2\pi m / D_x , \qquad (4\text{-a})$$

$$k_{yn} = k_0 \sin\theta_{inc} \sin\phi_{inc} + 2\pi n / D_y \,, \quad \text{(4-b)}$$

$$T_{mn} = \left(1/\sqrt{D_x D_y}\right)\exp(-jk_{xm}x - jk_{yn}y) \,, \quad \text{(4-c)}$$

$$k_{tmn} = \sqrt{k_{xm}^2 + k_{yn}^2} \,. \quad \text{(4-d)}$$

It should be noted that each value of the suffix (p) in (2) corresponds to a unique combination of m and n. The specular mode has the value of $p = p_{00}$ that corresponds to m=0 and n=0. By using these modal expansion functions of (3) in (2), one can obtain the transverse field components as follows:

$$E_x = \sum_p \frac{\left(\Phi_{(p)}^{TE} k_{y(p)} e^{-j\beta_{(p)}^{TE} z} + \Phi_{(p)}^{TM} k_{x(p)} e^{-j\beta_{(p)}^{TM} z}\right) T_{(p)}}{k_{t(p)}} \,, \quad \text{(5-a)}$$

$$E_y = \sum_p \frac{\left(-\Phi_{(p)}^{TE} k_{x(p)} e^{-j\beta_{(p)}^{TE} z} + \Phi_{(p)}^{TM} k_{y(p)} e^{-j\beta_{(p)}^{TM} z}\right) T_{(p)}}{k_{t(p)}} \,, \quad \text{(5-b)}$$

$$H_x = \sum_p \frac{\left(C_{(p)}^{TE} k_{x(p)} e^{-j\beta_{(p)}^{TE} z} - C_{(p)}^{TM} k_{y(p)} e^{-j\beta_{(p)}^{TM} z}\right) T_{(p)}}{k_{t(p)}} \,, \quad \text{(5-c)}$$

$$H_y = \sum_p \frac{\left(C_{(p)}^{TE} k_{y(p)} e^{-j\beta_{(p)}^{TE} z} + C_{(p)}^{TM} k_{x(p)} e^{-j\beta_{(p)}^{TM} z}\right) T_{(p)}}{k_{t(p)}} \,, \quad \text{(5-d)}$$

where

$$T_{(p)} = \left(1/\sqrt{D_x D_y}\right)\exp(-jk_{x(p)}x - jk_{y(p)}y) \,, \quad \text{(6-a)}$$

$$k_{t(p)} = \sqrt{k_{x(p)}^2 + k_{y(p)}^2} \,. \quad \text{(6-b)}$$

The constitutive relations in a chiral medium can be presented as:

$$\mathbf{D} = \varepsilon_0 \varepsilon_r \mathbf{E} - j\kappa\sqrt{\mu_0 \varepsilon_0}\,\mathbf{H} \,, \quad \text{(7-a)}$$

$$\mathbf{B} = \mu_0 \mu_r \mathbf{H} + j\kappa\sqrt{\mu_0 \varepsilon_0}\,\mathbf{E} \,, \quad \text{(7-b)}$$

where κ is the chirality coefficient. Based on these constitutive relations, one can obtain the longitudinal field components in terms of the longitudinal electric and magnetic flux densities as follows:

$$E_z = \left[(\mu_r/\varepsilon_0) D_z + \left(j\kappa/\sqrt{\mu_0 \varepsilon_0}\right) B_z\right]/\xi \,, \quad \text{(8-a)}$$

$$H_z = -\left[\left(j\kappa/\sqrt{\mu_0 \varepsilon_0}\right) D_z - (\varepsilon_r/\mu_0) B_z\right]/\xi \,, \quad \text{(8-b)}$$

where $\xi = \mu_r \varepsilon_r - \kappa^2$. By applying Maxwell's curl equations, one can obtain these longitudinal electric and magnetic flux densities as functions of the derivatives of the transverse electric and magnetic field components as follows:

$$E_z = \frac{1}{j\omega\xi}\left[\frac{\mu_r}{\varepsilon_0}\left(\frac{\partial H_y}{\partial x} - \frac{\partial H_x}{\partial y}\right) - \frac{j\kappa}{\sqrt{\mu_0 \varepsilon_0}}\left(\frac{\partial E_y}{\partial x} - \frac{\partial E_x}{\partial y}\right)\right], \quad \text{(9-a)}$$

$$H_z = \frac{-1}{j\omega\xi}\left[\frac{j\kappa}{\sqrt{\mu_0 \varepsilon_0}}\left(\frac{\partial H_y}{\partial x} - \frac{\partial H_x}{\partial y}\right) + \frac{\varepsilon_r}{\mu_0}\left(\frac{\partial E_y}{\partial x} - \frac{\partial E_x}{\partial y}\right)\right], \quad \text{(9-b)}$$

Thus, the problem is converted into finding out the transverse field component distribution where it would be required to determine the amplitudes of the transverse modes and the corresponding longitudinal propagation constants which are discussed in Eq. (2). To do this, it is required to formulate the problem as an eigenvalue problem where the amplitudes of the transverse modes correspond to the eigenvectors and the longitudinal propagation constants are the eigenvalues. This can be obtained by inserting the modal expansion of transverse field components in Maxwell's curl equations and weighting the resulting equations with P weighting functions. Based on the Galerkin's method and using the constitutive relations in (7), one can obtain that:

$$\left\langle j\omega D_x, T_{(q)}\right\rangle = \left\langle j\omega\left(\varepsilon_0\varepsilon_r E_x - j\kappa\sqrt{\mu_0\varepsilon_0}H_x\right), T_{(q)}\right\rangle = \left\langle \frac{\partial H_z}{\partial y} + \frac{\partial H_y}{\partial z}, T_{(q)}\right\rangle \,, \quad \text{(10-a)}$$

which can be represented in terms of the modal functions at $z = 0$ as follows:

$$\left\langle j\omega\begin{pmatrix} \varepsilon_0\varepsilon_r \sum_p \left[\left(\Phi_{(p)}^{TE} k_{y(p)} + \Phi_{(p)}^{TM} k_{x(p)}\right) T_{(p)}\right]/k_{t(p)} \\ -j\kappa\sqrt{\mu_0\varepsilon_0}\sum_p \left[\left(C_{(p)}^{TE} k_{x(p)} - C_{(p)}^{TM} k_{y(p)}\right) T_{(p)}\right]/k_{t(p)} \end{pmatrix}, T_{(q)}\right\rangle - \left\langle \frac{\partial}{\partial y}\begin{bmatrix} -\frac{\varepsilon_r}{\omega\xi\mu_0}\sum_p \Phi_{(p)}^{TE} k_{t(p)} T_{(p)} \\ + j\frac{\kappa}{\omega\xi\sqrt{\mu_0\varepsilon_0}}\sum_p C_{(p)}^{TM} k_{t(p)} T_{(p)} \end{bmatrix}, T_{(q)}\right\rangle$$
$$= j\beta_{(q)}^{TE} C_{(q)}^{TE} k_{y(q)}/k_{t(q)} + j\beta_{(q)}^{TM} C_{(q)}^{TM} k_{x(q)}/k_{t(q)} \,, \quad \text{(10-b)}$$

where the inner product is defined as:

$$\langle f, g\rangle = \int_{-D_y/2}^{D_y/2}\int_{-D_x/2}^{D_x/2} f(x,y) g^*(x,y)\,dx\,dy \,. \quad \text{(10-c)}$$

By following similar steps, one can obtain equations for D_y, B_x, and B_y. By arranging these equations, one can obtain the following eigenvalue problem:

$$\begin{bmatrix} [L_{HH}^{TE/TE}]_{P\times P} & [L_{HH}^{TE/TM}]_{P\times P} & [L_{HE}^{TE/TE}]_{P\times P} & [L_{HE}^{TE/TM}]_{P\times P} \\ [L_{HH}^{TM/TE}]_{P\times P} & [L_{HH}^{TM/TM}]_{P\times P} & [L_{HE}^{TM/TE}]_{P\times P} & [L_{HE}^{TM/TM}]_{P\times P} \\ [L_{EH}^{TE/TE}]_{P\times P} & [L_{EH}^{TE/TM}]_{P\times P} & [L_{EE}^{TE/TE}]_{P\times P} & [L_{EE}^{TE/TM}]_{P\times P} \\ [L_{EH}^{TM/TE}]_{P\times P} & [L_{EH}^{TM/TM}]_{P\times P} & [L_{EE}^{TM/TE}]_{P\times P} & [L_{EE}^{TM/TM}]_{P\times P} \end{bmatrix} \begin{bmatrix} C^{TE} \\ C^{TM} \\ \Phi^{TE} \\ \Phi^{TM} \end{bmatrix}$$
$$= \begin{bmatrix} [j\beta^{TE}] & 0 & 0 & 0 \\ 0 & [j\beta^{TM}] & 0 & 0 \\ 0 & 0 & [j\beta^{TE}] & 0 \\ 0 & 0 & 0 & [j\beta^{TM}] \end{bmatrix} \begin{bmatrix} C^{TE} \\ C^{TM} \\ \Phi^{TE} \\ \Phi^{TM} \end{bmatrix}, \quad (11)$$

where the elements of this eigenvalue problem are presented in Appendix (I). It should be noted that the dimension of this eigenvalue problem is $4P \times 4P$ which introduces $2P$ forward modes and $2P$ backward modes.

B. Mode matching analysis of chiral grating structures

By using the mode matching technique and following the same steps in [15], one can obtain the general scattering matrix between two semi-infinite chiral gratings of the same periodicity and coincide at the plane z=0 as follows:

$$\mathbf{S} = \left(\mathbf{B}^T\right)^{-1}\mathbf{A}$$
$$= \begin{bmatrix} \begin{bmatrix} [S_{11}^{TE/TE}] & [S_{11}^{TE/TM}] \\ [S_{11}^{TM/TE}] & [S_{11}^{TM/TM}] \end{bmatrix} & \begin{bmatrix} [S_{12}^{TE/TE}] & [S_{12}^{TE/TM}] \\ [S_{12}^{TM/TE}] & [S_{12}^{TM/TM}] \end{bmatrix} \\ \begin{bmatrix} [S_{21}^{TE/TE}] & [S_{21}^{TE/TM}] \\ [S_{21}^{TM/TE}] & [S_{21}^{TM/TM}] \end{bmatrix} & \begin{bmatrix} [S_{22}^{TE/TE}] & [S_{22}^{TE/TM}] \\ [S_{11}^{TM/TE}] & [S_{22}^{TM/TM}] \end{bmatrix} \end{bmatrix}, \quad (12)$$

where

$$\mathbf{A} = \begin{bmatrix} [\Phi_a^{TE}]^T & [\Phi_a^{TM}]^T & [C_a^{TE}]^T & [C_a^{TM}]^T \\ [-\Phi'^{TE}_a]^T & [-\Phi'^{TM}_a]^T & [-C'^{TE}_a]^T & [-C'^{TM}_a]^T \end{bmatrix}, \quad (13\text{-a})$$

$$\mathbf{B} = \begin{bmatrix} [-\Phi'^{TE}_b]^T & [-\Phi'^{TM}_b]^T & [-C'^{TE}_b]^T & [-C'^{TM}_b]^T \\ [\Phi_b^{TE}]^T & [\Phi_b^{TM}]^T & [C_b^{TE}]^T & [C_b^{TM}]^T \end{bmatrix}. \quad (13\text{-b})$$

The suffixes a and b in (13) correspond to the upper and the lower grating, respectively. The primed terms correspond to the backward propagating modes while the terms without a prime correspond to forward propagating modes. For a special case where the upper limit is free space, the parameters of the upper grating structure are $\varepsilon_{rb} = \varepsilon_{ri} = 1$, $\mu_{rb} = \mu_{ri} = 1$ and $\kappa_{rb} = \kappa_{ri} = 1$.

For the case of a finite-thickness chiral grating slab of thickness h, the total reflection and transmission coefficients can be obtained in terms of generalized scattering matrices as follows [5]:

$$[\widetilde{R}_{11}] = [S_{11}] + [S_{12}](I - [\Lambda][S_{22}][\Lambda'][S_{22}])^{-1}[\Lambda'][S_{22}][\Lambda][S_{21}], \quad (14\text{-a})$$
$$[\widetilde{T}_{12}] = [S_{12}](I - [\Lambda][S_{22}][\Lambda'][S_{22}])^{-1}[\Lambda][S_{21}], \quad (14\text{-b})$$

where

$$[S_{ij}] = \begin{bmatrix} [S_{ij}^{TE/TE}] & [S_{ij}^{TE/TM}] \\ [S_{ij}^{TM/TE}] & [S_{ij}^{TM/TM}] \end{bmatrix}, \quad (15\text{-a})$$

which corresponds to the generalized scattering matrices of the semi-infinite chiral grating in (11) where the upper medium is free space. On the other hand $[\Lambda]$ and $[\Lambda']$ correspond to the forward and backward phase delay matrices as follows:

$$[\Lambda] = \begin{bmatrix} [\exp(-j\beta^{TE}h)] & 0 \\ 0 & [\exp(-j\beta^{TM}h)] \end{bmatrix}, \quad (15\text{-b})$$
$$[\Lambda'] = \begin{bmatrix} [\exp(-j\beta'^{TE}h)] & 0 \\ 0 & [\exp(-j\beta'^{TM}h)] \end{bmatrix}. \quad (15\text{-c})$$

Finally, I in (14) corresponds to a unit matrix of dimension $2P \times 2P$.

The reflection and transmission matrices of Eq. (14) represent the reflection and transmission of P TE and P TM modes and the interaction between them. Specular reflection and transmission coefficients can be obtained by selecting the corresponding terms in the generalized reflection and transmission matrices of (14). Thus the specular TE reflection coefficient due to the TE incident wave is obtained as $R_{11}^{TE/TE} = \widetilde{R}_{11}[p_{00}][p_{00}]$ where $p = p_{00}$ corresponds to the Floquet mode m=0 and n=0 as discussed earlier. On the other hand the specular TE reflection coefficient due to the TM incident wave is obtained as $R_{11}^{TE/TM} = \widetilde{R}_{11}[p_{00}][p_{00}+P]$. Similarly, the specular TM reflection coefficients due to TE and TM incident waves are obtained as $R_{11}^{TM/TE} = \widetilde{R}_{11}[p_{00}+P][p_{00}]$ and $R_{11}^{TM/TM} = \widetilde{R}_{11}[p_{00}+P][p_{00}+P]$, respectively. In a similar way, one can obtain the sepcular transmission coefficients as $T_{12}^{TE/TE} = \widetilde{T}_{12}[p_{00}][p_{00}]$, $T_{12}^{TE/TM} = \widetilde{T}_{12}[p_{00}][p_{00}+P]$, $T_{12}^{TM/TE} = \widetilde{T}_{12}[p_{00}+P][p_{00}]$, and $T_{12}^{TM/TM} = \widetilde{T}_{12}[p_{00}+P][p_{00}+P]$. It should be noted that these coefficients correspond to the complex reflection and transmission coefficients of the electric field components. The corresponding power reflection and transmission coefficients are obtained as the square value of the amplitudes of these electric field coefficients. For the sake of comparison with the available previously published results, we present the results of power reflection and transmission coefficients as it is discussed in the following section.

III. RESULTS AND DISCUSSIONS

In this section, we present sample results to verify the present analysis. It should be noted that the present method represents a general form for the cases of dielectric and magneto-dielectric grating slabs by setting the chirality coefficients in both the base substrate and the implanted rods to be zero. This method can also be used for both one-dimensional and two-dimensional grating. For the case of one-dimensional grating, the length of the implanted rod in one direction is extended to be the same as the periodic distance in this direction. For the space limit, we did not show comparisons with previously published results of dielectric grating and magneto-dielectric grating. However, we obtained excellent agreement with these results.

It should be noted that the presented results are based on normalized dimensions with respect to the operating wavelength. Thus, these results are not limited for a certain frequency. The present analysis has no lower limit on the normalized dimensions. However, for the case of a chiral grating slab with a quite small periodic cell compared with the operating wavelength, we obtained reflection and transmission coefficients which are nearly the same as the corresponding ones of a homogenous chiral slab having electrical properties equivalent to the average properties of the host and inclusion as discussed in [4]. This average in the present case is obtained based on the ratio of the dimensions of both the inclusion and the host in the unit cell. This property has been quite clarified in [4], thus these results are not repeated here. On the other hand, the upper limit of the normalized dimensions of the cells is kept below unity to avoid the presence of higher order propagating Floquet modes in air-side as discussed in [4].

For the case of a one-dimensional chiral grating slab, we present a sample result for comparison with the published results of Wu and Jaggard [4]. In this case, the parameters of the base and inclusion are $\varepsilon_{rb} = 2.5, \mu_{rb} = 1, \kappa_b = 0.1$ and $\varepsilon_{r1} = 1.5, \mu_{r1} = 1, \kappa_1 = 0.1$, respectively. The periodic cell is square and is related to the grating thickness as $D_x = D_y = h/1.713$. The dimensions of the implanted rod inside the cell are $L_x = D_x/2$ and $L_y = D_y$. The incident plane wave is assumed to be the TE wave of incidence angle $\theta_{inc} = 45^\circ$, $\phi_{inc} = 0^\circ$. Figure 2 shows the specular reflection and transmission coefficients in this case for both the co-polarized and cross-polarized components as functions of normalized grating thickness where $k_0 = 2\pi/\lambda_0$ corresponds to the free space wave number. By comparing this figure with the corresponding results in [4], one obtains an excellent agreement.

In this paper, we extend the previous case to be a two-dimensional chiral grating by setting $L_y = D_y/2$. We also changed the permeability of the base to be $\mu_{rb} = 1.4$. The remaining parameters are the same as in Fig. 2. We studied both TE and TM cases as shown in Figure 3 and 4. It can be noted that the polarization conversion in the reflected field is greater at resonance frequencies in the case of TE incident wave than the case of TM incident wave.

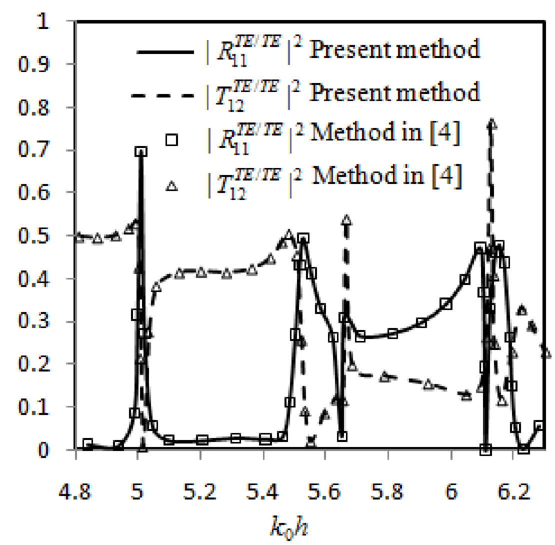

(a) TE reflection and transmission coefficients due to TE incident wave.

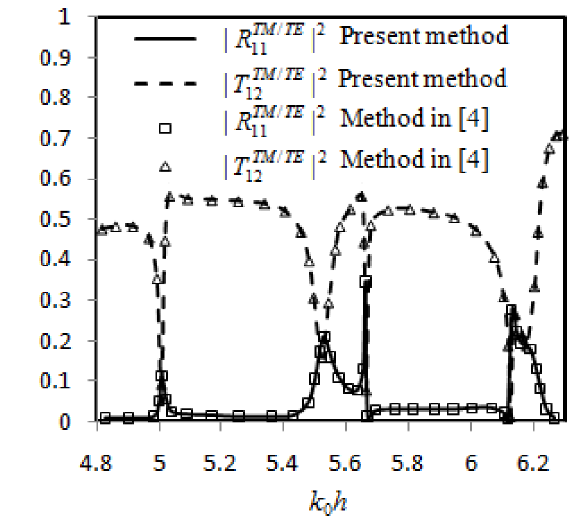

(b) TM reflection and transmission coefficients due to TE incident wave.

Fig. 2. Specular power reflection and transmission coefficients due to an obliquely incident TE plane wave on a chiral grating slab. $\theta_{inc} = 45^\circ$, . $\phi_{inc} = 0^\circ$, $\varepsilon_{rb} = 2.5$, , $\mu_{rb} = 1$, $\kappa_b = 0.1$, $\varepsilon_{r1} = 1.5$, $\mu_{r1} = 1$, $\kappa_1 = 0.1$, $D_x = D_y = h/1.713$, $L_x = D_x/2$ and $L_y = D_y$.

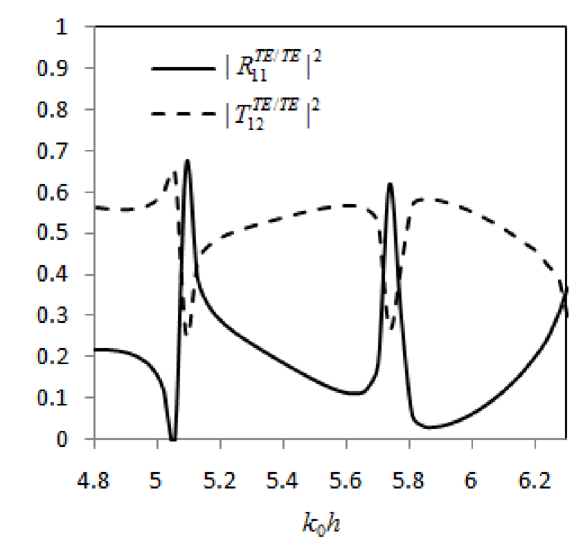

(a) TE reflection and transmission coefficients due to TE incident wave.

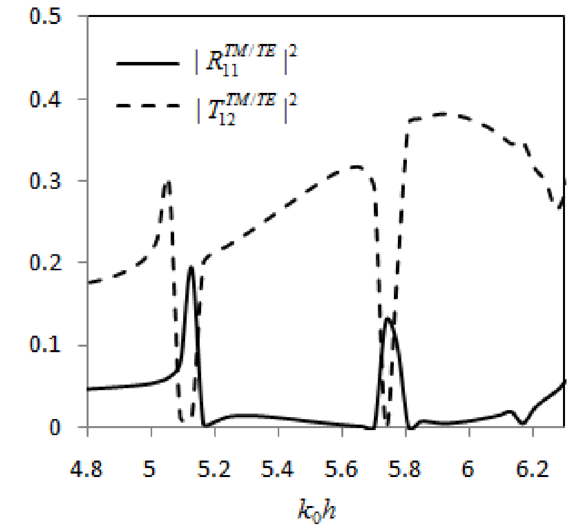

(b) TM reflection and transmission coefficients due to TE incident wave.

Fig. 3. Specular power reflection and transmission coefficients due to an obliquely incident TE plane wave on a chiral grating slab. $\theta_{inc} = 45^\circ$, $\phi_{inc} = 0^\circ$, $\varepsilon_{rb} = 2.5$, $\mu_{rb} = 1.4$, $\kappa_b = 0.1$, $\varepsilon_{r1} = 1.5$, $\mu_{r1} = 1$, $\kappa_1 = 0.1$, $D_x = D_y = h/1.713$, $L_x = D_x/2$ and $L_y = D_y/2$.

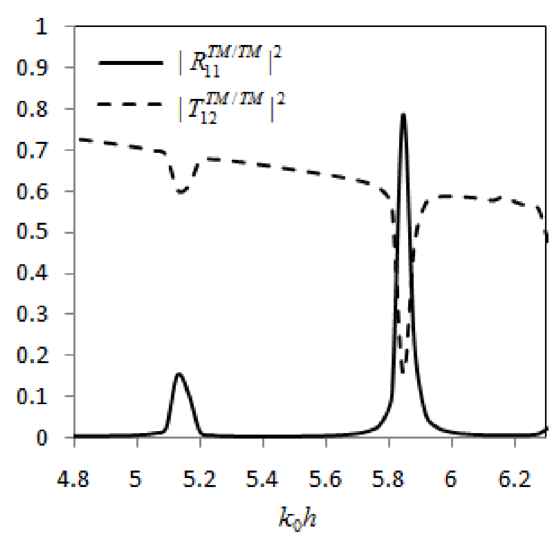

(a) TM reflection and transmission coefficients due to TM incident wave.

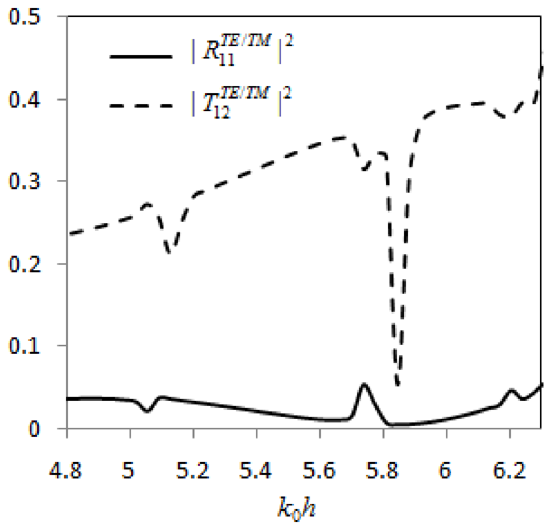

(b) TE reflection and transmission coefficients due to TM incident wave.

Fig. 4. Specular power reflection and transmission coefficients due to an obliquely incident TM plane wave on a chiral grating slab for the same parameters of Fig. 3.

IV. CONCLUSION

Chiral grating can be used to control both the magnitude and polarization of the reflected and transmitted fields. In this paper, we presented detailed modal analysis of two-dimensional chiral grating. This modal analysis is combined with mode matching technique and generalized matrix method to study the reflection and transmission due to a finite thickness two-dimensional chiral grating slab. The present analysis represents a generalization for previously studied cases including dielectric grating, magneto-dielectric grating and one-dimensional chiral grating.

APPENDIX (I)

The details of the elements of the eigenvalue problem in Eq. (11) are presented in this Appendix. These elements are obtained as:

$$l_{HH(q)(p)}^{TE/TE} = l_{EE(q)(p)}^{TM/TM} = \\ = \frac{k_0\left(k_{x(p)}k_{y(q)} - k_{y(p)}k_{x(q)}\right)}{k_{t(p)}k_{t(q)}}\left\langle \kappa T_{(p)}, T_{(q)}\right\rangle . \quad \text{(A-1)}$$

$$l_{HH(q)(p)}^{TE/TM} = -l_{EE(q)(p)}^{TM/TE} = \\ = -\frac{k_0\left(k_{x(p)}k_{x(q)} + k_{y(p)}k_{y(q)}\right)}{k_{t(p)}k_{t(q)}}\left\langle \kappa T_{(p)}, T_{(q)}\right\rangle \\ - j\frac{k_{y(q)}k_{t(p)}}{k_0k_{t(q)}}\left\langle \frac{\partial}{\partial y}\left(\frac{\kappa}{\xi}T_{(p)}\right), T_{(q)}\right\rangle \\ - j\frac{k_{x(q)}k_{t(p)}}{k_0k_{t(q)}}\left\langle \frac{\partial}{\partial x}\left(\frac{\kappa}{\xi}T_{(p)}\right), T_{(q)}\right\rangle . \quad \text{(A-2)}$$

$$l_{HE(q)(p)}^{TE/TE} = \frac{jk_0\left(k_{x(p)}k_{x(q)} + k_{y(p)}k_{y(q)}\right)}{Z_0k_{t(p)}k_{t(q)}}\left\langle \varepsilon_r T_{(p)}, T_{(q)}\right\rangle \\ + \frac{k_{x(q)}k_{t(p)}}{k_0Z_0k_{t(q)}}\left\langle \frac{\partial}{\partial x}\left(\frac{\varepsilon_r}{\xi}T_{(p)}\right), T_{(q)}\right\rangle \\ + \frac{k_{y(q)}k_{t(p)}}{k_0Z_0k_{t(q)}}\left\langle \frac{\partial}{\partial y}\left(\frac{\varepsilon_r}{\xi}T_{(p)}\right), T_{(q)}\right\rangle . \quad \text{(A-3)}$$

$$l_{HE(q)(p)}^{TE/TM} = \frac{jk_0\left(k_{x(p)}k_{y(q)} - k_{y(p)}k_{x(q)}\right)}{Z_0k_{t(p)}k_{t(q)}}\left\langle \varepsilon_r T_{(p)}, T_{(q)}\right\rangle . \quad \text{(A-4)}$$

$$l_{HH(q)(p)}^{TM/TE} = -l_{EE(q)(p)}^{TE/TM} \\ = \frac{k_0\left(k_{x(p)}k_{x(q)} + k_{y(p)}k_{y(q)}\right)}{k_{t(p)}k_{t(q)}}\left\langle \kappa T_{(p)}, T_{(q)}\right\rangle . \quad \text{(A-5)}$$

$$l_{HH(q)(p)}^{TM/TM} = l_{EE(q)(p)}^{TE/TE} \\ = -\frac{k_0\left(k_{y(p)}k_{x(q)} - k_{x(p)}k_{y(q)}\right)}{k_{t(p)}k_{t(q)}}\left\langle \kappa T_{(p)}, T_{(q)}\right\rangle \\ - j\frac{k_{x(q)}k_{t(p)}}{k_0k_{t(q)}}\left\langle \frac{\partial}{\partial y}\left(\frac{\kappa}{\xi}T_{(p)}\right), T_{(q)}\right\rangle \\ + j\frac{k_{y(q)}k_{t(p)}}{k_0k_{t(q)}}\left\langle \frac{\partial}{\partial x}\left(\frac{\kappa}{\xi}T_{(p)}\right), T_{(q)}\right\rangle . \quad \text{(A-6)}$$

$$l_{HE(q)(p)}^{TM/TE} = \frac{jk_0\left(k_{y(p)}k_{x(q)} - k_{x(p)}k_{y(q)}\right)}{Z_0k_{t(p)}k_{t(q)}}\left\langle \varepsilon_r T_{(p)}, T_{(q)}\right\rangle \\ + \frac{k_{x(q)}k_{t(p)}}{k_0Z_0k_{t(q)}}\left\langle \frac{\partial}{\partial y}\left(\frac{\varepsilon_r}{\xi}T_{(p)}\right), T_{(q)}\right\rangle \\ - \frac{k_{y(q)}k_{t(p)}}{k_0Z_0k_{t(q)}}\left\langle \frac{\partial}{\partial x}\left(\frac{\varepsilon_r}{\xi}T_{(p)}\right), T_{(q)}\right\rangle . \quad \text{(A-7)}$$

$$l_{HE(q)(p)}^{TM/TM} = \frac{jk_0\left(k_{x(p)}k_{x(q)} + k_{y(p)}k_{y(q)}\right)}{Z_0k_{t(p)}k_{t(q)}}\left\langle \varepsilon_r T_{(p)}, T_{(q)}\right\rangle . \quad \text{(A-8)}$$

$$l_{EH(q)(p)}^{TE/TE} = \frac{jk_0Z_0\left(k_{x(p)}k_{x(q)} + k_{y(p)}k_{y(q)}\right)}{k_{t(p)}k_{t(q)}}\left\langle \mu_r T_{(p)}, T_{(q)}\right\rangle . \quad \text{(A-9)}$$

$$l_{EH(q)(p)}^{TE/TM} = jk_0 Z_0 \frac{\left(k_{x(p)}k_{y(q)} - k_{y(p)}k_{x(q)}\right)}{k_{t(p)}k_{t(q)}} \left\langle \mu_r T_{(p)}, T_{(q)} \right\rangle + \frac{Z_0 k_{t(p)} k_{y(q)}}{k_0 k_{t(q)}} \left\langle \frac{\partial}{\partial x}\left(\frac{\mu_r}{\xi} T_{(p)}\right), T_{(q)} \right\rangle - \frac{Z_0 k_{t(p)} k_{x(q)}}{k_0 k_{t(q)}} \left\langle \frac{\partial}{\partial y}\left(\frac{\mu_r}{\xi} T_{(p)}\right), T_{(q)} \right\rangle. \quad \text{(A-10)}$$

$$l_{EH(q)(p)}^{TM/TE} = \frac{jk_0 Z_0 \left(k_{y(p)}k_{x(q)} - k_{x(p)}k_{y(q)}\right)}{k_{t(p)}k_{t(q)}} \left\langle \mu_r T_{(p)}, T_{(q)} \right\rangle. \quad \text{(A-11)}$$

$$l_{EH(q)(p)}^{TM/TM} = jk_0 Z_0 \frac{\left(k_{x(p)}k_{x(q)} + k_{y(p)}k_{y(q)}\right)}{k_{t(p)}k_{t(q)}} \left\langle \mu_r T_{(p)}, T_{(q)} \right\rangle + \frac{Z_0 k_{t(p)} k_{x(q)}}{k_0 k_{t(q)}} \left\langle \frac{\partial}{\partial x}\left(\frac{\mu_r}{\xi} T_{(p)}\right), T_{(q)} \right\rangle + \frac{Z_0 k_{t(p)} k_{y(q)}}{k_0 k_{t(q)}} \left\langle \frac{\partial}{\partial y}\left(\frac{\mu_r}{\xi} T_{(p)}\right), T_{(q)} \right\rangle. \quad \text{(A-12)}$$

For the special case where the unit cell and implanted rod are of rectangular shapes as shown in Fig. 1, the above inner products can be obtained analytically in closed forms as discussed in [6].

REFERENCES

[1] V. R. Tuz and C.W. Qiu, "Semi-Infinite Chiral Nihility Photonics: Parametric Dependence, Wave Tunneling and Rejection," *Progress In Electromagnetics Research,* vol. PIER 103, pp. 139-152, 2010.

[2] D. L. Jaggard, N. Engheta, M. W. Kowarz, P. Pelet, J. C. Liu, and Y. Kim, "Periodic Chiral Structures," *IEEE Trans. Antennas Propagat.*, vol. AP-37, pp. 1447–1452, 1989.

[3] L. G. Zheng and W. X. Zhang, "Analysis of Bi-Anisotropic PBG Structure using Plane Wave Expansion Method," *Progress In Electromagnetics Research,* vol. PIER 42, pp. 233–246, 2003.

[4] T. X. Wu and D. L. Jaggard, "Scattering of Chiral Periodic Structure," *IEEE Trans. Antennas Propagat.*, vol. AP-52, pp. 1859-1870, 2004.

[5] A. M. Attiya and A. A. Kishk, "Modal Analysis of a Two-Dimensional Dielectric Grating Slab Excited by an Obliquely Incident Plane Wave," *Progress In Electromagnetics Research,* vol. PIER 60, pp. 221–243, 2006.

[6] A. M . Attiya, A. A. Kishk, and A. W. Glisson, "Analysis of Two-Dimensional Magneto-Dielectric Grating Slab," *Progress In Electromagnetics Research,* vol. PIER 74, pp.195–216, 2007.

[7] A. Lakhtakia, "On a Fourth-Order Wave Equation for EM Propagation in Chiral Media," *Appl. Phys.* B, vol. 36, pp.163-165, 1985.

[8] A. Gomez, I. Barba, A. C. L. Cabeceira, J. Represa, A. Vegas, and M. A. Solano, "Electromagnetic Propagation in Unbounded Inhomogeneous Chiral Media using the Coupled Mode Method," *Microwave Opt.Technol. Lett.* vol. 49, pp. 2771-2779, 2007.

[9] A. Gomez, A. Vegas, and M. A. Solano, "On Two Different Formulations of the Coupled Mode Method: Application to 3D Rectangular Chirowaveguides," *Int. J. Electron. Commun.* vol. (AEU) 60, pp. 690–704, 2006.

[10] A. Gomez, A. Lakhtakia, A. Vegas, and M. A. Solano, "Hybrid Technique for Analysing Metallic Waveguides Containing Isotropic Chiral Materials," *IET Microw. Antennas Propag.*, vol. 4, pp. 305–315, 2010.

[11] T. X. Wu and D. L. Jaggard, "A Comprehensive Study of Discontinuities in Chirowaveguides," *IEEE Trans. Microw. Theory Tech.*, vol. MTT-50, pp. 2320–2330, 2002.

[12] J. Pitarch, J. M. Catal-Civera, F. L. Pen Aranada-Foix, and M. A. Solano, "Efficient Modal Analysis of Bianisotropic Waveguides by the Coupled Mode Method," *IEEE Trans. Microwave Theory Tech.*, vol. MTT-55, pp. 108–116, 2007.

[13] A. Gomez , A. Lahktakia, and J. Magineda "Full-Wave Hybrid Technique for 3D Isotropic-Chiral-Material Discontinuities in Rectangular Waveguides: Theory and Experiment," *IEEE Trans. Microwave Theory Tech.*, vol. MTT-56, pp. 2815–2825, 2008.

[14] S. T. Imeci, F. Altunkilic, J. R. Mautz, and E. Arvas, "Transmission Through an Arbitrarily Shaped Aperture in a Conducting Plane Separating Air and a Chiral Medium," *Applied Computational Electromagnetic Society (ACES) Journal*, vol.25, pp. 587–599, July 2010.

[15] M. A. Solano, A. Vegas, and A. Prieto, "Numerical Analysis of Discontinuities in a Rectangular Waveguide Loaded with Isotropic or Anisotropic Obstacles by Means of the Coupled-Mode Method and the Mode-Matching Method," *Int. J. Numer. Model.:*

Electron. Netw. Dev. Fields, vol. 7, pp. 433–452, 1994.

Ahmed M. Attiya graduated from Zagazig University of Egypt in 1991 and received the M.Sc. and Ph.D. in Electronics and Electrical Communications from Cairo University in 1996 and 2001, respectively. Attiya is an Associate Prof. in the Microwave Engineering Dept. Electronics Research Institute. In 2002-2004, he was a research fellow in Virginia Polytechnic Inst. and State Univ. In 2004-2005, he was a visiting scholar in University of Mississippi. His research interest includes antennas, electromagnetic wave propagation, scattering and diffraction problems, and numerical techniques in electromagnetics.